Hydration dynamics of human fingernails: An ellipsometric study

B. Schulz, D. Chan, J. Bäckström, and M. Rübhausen
Institut für Angewandte Physik und Zentrum für Mikrostrukturforschung, Universität Hamburg, Jungiusstraße 11, D-20355 Hamburg, Germany

K. P. Wittern, S. Wessel, and R. Wepf
Beiersdorf AG, Unnastraße 48, D-20245 Hamburg, Germany

S. Williams
Fachbereich Chemie, Kosmetik und Körperpflege, Universität Hamburg, Von-Melle-Park 8, D-20146 Hamburg, Germany
(Received 28 February 2002; published 25 June 2002; publisher error corrected 2 July 2002)

We use spectroscopic ellipsometry to obtain the complex refractive index, $\tilde{n}=n+ik$, of human fingernails. By studying the change of $\tilde{n}$ upon hydration and dehydration, we reveal three different time domains with typical time constants of 4, 150, and 3200 min. A simple model that takes into account the presence of one fast and one slow process is fully consistent with the observed hydration and dehydration dynamics. We attribute these processes to ''free'' water incorporated between the keratin filaments and water more tightly ''bound'' in keratin complexes, respectively. From our model we determine the hydration profiles of ''free'' and ''bound'' water during, both, hydration and dehydration.

DOI: 10.1103/PhysRevE.65.061913 PACS number(s): 87.15.He, 07.60.Fs, 87.64.Aa, 87.64.Ni

I. INTRODUCTION

Optical studies on complex biological systems have become increasingly important during the last two decades [1,2]. However, mostly techniques using diffuse light [2] such as reflectometry or transmission measurements have been used to study the optical properties of biological matter such as nails, skin, muscle fibers, and liver tissue [2,3]. Many models of the complex refractive index (that determines the optical properties), and its dependence on the chemistry and the morphology of biological tissue have emerged and have hardly been tested experimentally [4]. Furthermore, many of the applied experimental techniques are destructive to the investigated material so that a straightforward comparison between theoretical models and experimental facts is often not feasible. As an example, the hydration dynamics of human nails have been investigated by Raman spectroscopy, but due to the strong heating of the sample by the laser beam no dehydration process could be measured [5].

Ellipsometry is an optical technique that determines amplitude and phase changes denoted as two quantities Ψ and Δ, respectively, upon reflection of light from a sample [6]. From these two quantities, one can unambiguously deduce the complex refractive index $\tilde{n}=n+ik$ for a homogeneous, semi-infinite system [6]. To our knowledge, only a few ellipsometry studies of biological tissues and bio-organic materials have been published [7–9].

There are still many open questions regarding the optical properties of human nails, such as the complex refractive index, scattering properties, or scattering phase functions [10]. The optical properties should be determined by the main components keratin, lipids, water, and trace elements, such as calcium, potassium, sodium, and magnesium. Like all proteins, the structure of keratin can be described as follows. First, the primary structure is determined by the sequence of the single amino acids, which result in the polypeptide, the protein. The secondary structure is given by specific foldings of the chain due to the interactions of the amino acids resulting in, e.g., α helices or β sheets. These secondary structures of the protein group together due to hydrophobic interactions between side chains of the amino acids and form the tertiary structure [11]. The quartenary structure is the combination of eight proteins forming a keratin filament. Any changes in these structures can affect the optical properties via changes in the electronic configuration. Also the morphology, given by the orientation of the keratin filaments inside the nail, should influence the optical properties [12].

Here, we show that ellipsometry using focused light is an excellent tool to determine the optical properties of nails. We are able to gain information about the water content of the nail to study its hydration dynamics. The time evolution of the optical parameters follows an exponential behavior. We have determined one time constant of $\tau_1=4$ min during hydration, but two, namely, $\tau_2=150$ and $\tau_3=3200$ min during dehydration. To analyze the time dependence of the optical properties during hydration and dehydration, we employ a model describing the water exchange within the nail. Water molecules can be either regarded as ''free'' or ''bound'' with respect to the keratin matrix structure of the nail. We derive the time behavior of both types of water. The optical constants n and k are computed with the help of an effective medium approximation [6]. The resulting time dependence of the refractive index and the absorption coefficient agrees to a high degree with the experimental data.

II. EXPERIMENT

In ellipsometry, circularly or linearly polarized light is reflected under an angle of incidence ϕ_0 from the sample. The polarization properties of the directly reflected light are

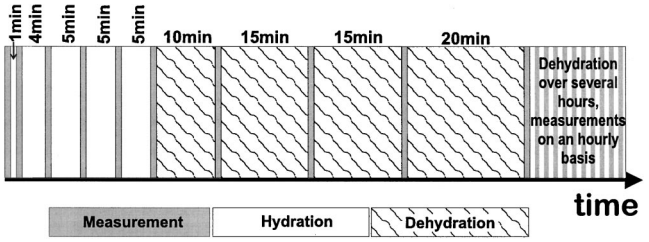

FIG. 1. Time schedule for the hydration and dehydration studies. The time required to perform one measurement is 38 s.

determined using a rotatable analyzer. The measured intensity for various analyzer positions is converted into the ellipsometric parameters Ψ and Δ. As we only measure relative changes of Ψ and Δ, this technique is self-normalizing in the sense that no reference spectrum is needed and that intensity fluctuations of, e.g., the light source cancel out. Assuming a homogeneous, semi-infinite material in air, the ellipsometric parameters Ψ and Δ can be straightforwardly transformed into the refractive index n and the absorption coefficient k [6],

$$\tilde{n} = \tan\phi_0 \left[1 - \frac{4\tan\Psi e^{i\Delta}}{(1+\tan\Psi e^{i\Delta})^2} \sin^2\phi_0 \right]^{1/2}. \qquad (1)$$

The angle of incidence was kept at 70° in our experiments. The experiments were performed with a SENTECH SE850 ellipsometer located in a clean room with controlled temperature ($20.0\,^{\circ}\mathrm{C} \pm 0.5\,^{\circ}\mathrm{C}$) and relative humidity ($40\% \pm 3\%$). The incident light is produced with a broadband xenon gas-discharge lamp, and the reflected light is recorded using a grating spectrograph and a photodiode array. The ellipsometer covers a spectral range between 230–780 nm in a single measurement. Because of the high surface roughness, we used focusing optics to focus the parallel beam of the ellipsometer with a diameter of ≈ 6 mm down to a spot with ≈ 200 μm diameter. The reflected light is collected and collimated into a parallel beam before passing the analyzer [13].

Nail clippings from different volunteers were measured on various positions in order to check the nail for homogeneity and individual variations. The nail parts originated from the distal part of the index or ring fingernail. In this part, they are a few months to half a year old and no longer connected to the nail bed. The samples were cut off and divided into two parts to measure more than one hydration process on the same fingernail. They were gently cleaned with isopropanol and stored at room temperature in the dry clean room. The first spectra were accumulated one week after cutting off the samples. They then stayed one month under the above described conditions before the hydration studies were performed.

These hydration studies started with a measurement of the nonwatered fingernail. After soaking the sample in water with a constant temperature of $20\,^{\circ}\mathrm{C}$ for 1 min, we performed the second measurement. Subsequently, we increased the time interval to 4 min and 5 min, yielding a total hydration time of 20 min (see Fig. 1). In the following hour, the sample was dried in the 40% relative humidity of the clean room without moving it from the ellipsometer. During this dehydration process, spectra were accumulated after 10, 25, 40, and 60 min. Several samples were left in their position to measure long-time dehydration. In this case, spectra were accumulated on an hourly basis until a total dehydration time of 46 h was reached.

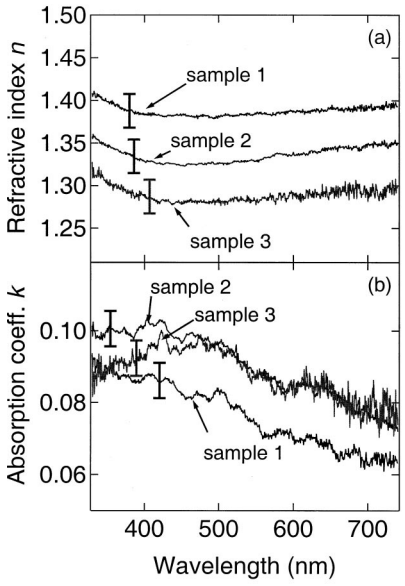

FIG. 2. Spectra of the optical constants n and k of several fingernails. Each curve represents the average of 12 spectra from different positions on the same sample. The samples were stored for one week at room temperature at 40% relative humidity.

III. RESULTS AND DISCUSSION

Figure 2 compares the refractive index and the absorption coefficient of three different nail samples. The data were obtained by averaging 12 spectra measured at different positions of the sample in order to minimize effects originating from inhomogeneous biological material arising from local chemical or morphological differences. At each position a slightly different combination of keratin, lipids, air, water, and trace elements, as well as a different spatial conformation of keratin filaments, results in slightly different optical properties. On every single position, the obtained spectra were reproducible within the noise of the setup. The error bars show the standard deviation of the absolute values of n and k due to this biological inhomogeneity. However, the line shape stays similar over the 12 positions. The absolute values of n for nail samples from different volunteers range between 1.25 and 1.40, which is more than the biological variations within one sample. This can be explained by individual variations, which derive from the fact that the keratin filament structure inside the nail is not the same among different persons. Differences can be caused by, e.g., diseases, nutrition, cosmetic treatment, stress, or genetic diversity [14], resulting in variations of the morphological or chemical structure of the nail.

Regarding the absorption coefficient in Fig. 2(b), one can see that all fingernails display similar spectra, despite the

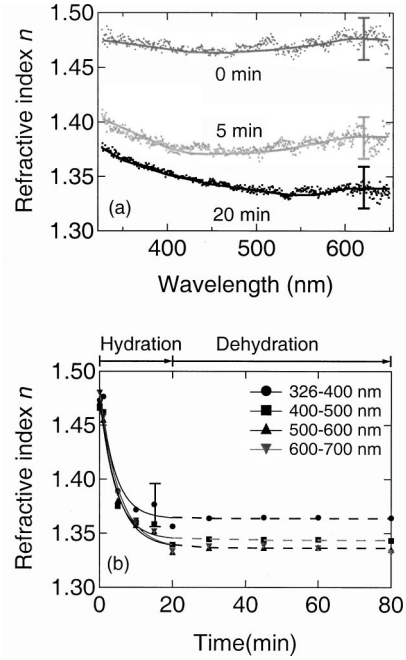

FIG. 3. (a) Refractive index n for a fingernail after different hydration times as indicated. Solid curves are guides to the eye. (b) Hydration and dehydration behavior of n in different spectral regions. The solid curves are exponential fits. Dashed lines are guides to the eye. The error bars are due to biological variations by the repositioning of the nail between hydrations. The sample was stored at room temperature for five weeks at 40% relative humidity.

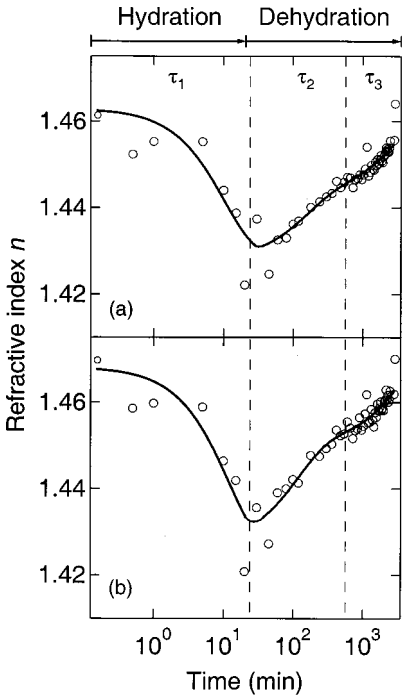

FIG. 4. Refractive index n for a fingernail sample on a logarithmic time scale for two spectral regions, (a) 400–500 nm and (b) 500–600 nm. Three different time domains are discernible in both regions. The solid curves are exponential fits. The sample was stored at room temperature for five weeks at 40% relative humidity.

individual variations. The line shape of k shows spectral features, which are only a little broadened by the averaging process. However, the curve for the refractive index in Fig. 2(a) is relatively smooth. Our results in Fig. 2 demonstrate overall the excellent signal to noise ratio of ellipsometry and its sensitivity to individual variations between different persons.

Figure 3 shows the results of the hydration dynamics in one representative sample that was additionally dried for four weeks in the clean room environment at 40% relative humidity. The spectra in Fig. 3(a) are single, not averaged data after 0, 5, and 20 min in the hydration protocol (see Fig. 1). The size of the error bars is estimated by biological variations due to the repositioning of the nail. The nonwatered sample displays a flat curve with a nearly constant refractive index around 1.47. After 5 min of hydration of the nail, the absolute values of n drop drastically over the whole spectral range and are between 1.40 and 1.37. However, it is already visible that the refractive index has dropped less in the ultraviolet region around 300 nm than in the region between 500 and 650 nm. The spectra accumulated after 20 min of hydration again show an increased slope and a decrease in the absolute values of n over the whole spectral range. One can now clearly see that the strongest decrease occurs in the energy region between 500 and 650 nm, whereas the energy region around 300 nm seems to saturate earlier.

In Fig. 3(b), the behavior of the refractive index over a hydration/dehydration schedule over 80 min is presented. Averages over the refractive index in various spectral regions are compared. As long as the sample is being hydrated, n is decreasing, where the decrease in the energy region around 300 nm is less than the decrease in the region between 500 and 650 nm. The rate of the decrease is lowered towards the end of the hydration time. During the following dehydration, n stays constant within the next 60 min. The measurement data in Fig. 3(b) were fitted with an exponential curve

$$n = A + B \exp\left(-\frac{t}{\tau_1}\right). \tag{2}$$

In the nonwatered state, for $t=0$, the refractive index is $n = A + B = 1.48$. For $t \to \infty$, the refractive index approaches $A = 1.34$, which is relatively close to the refractive index of water, $n = 1.33$. The time constant τ_1 as well as the values of A and B are sample dependent. The time constant differs between 4 min for the ultraviolet region and 5 min for the visible and infrared spectral regions.

The ellipsometric results of long-time dehydration processes using another fingernail sample are presented in Figs. 4 and 5. In this study, all measurements were made on the same position. Therefore, no biological variations influence the experiment and the error is given by the size of the markers. In both figures, one can distinguish three time domains governed by the different time constants τ_1, τ_2, and τ_3. The refractive index decreases exponentially during the hydration process with a time constant of $\tau_1 \approx 10$ min, which is close to the 5 min value estimated in Fig. 3(b), considering biological and individual variations. The sample shows a high saturation value at the end of the hydration period. This means that the sample did not absorb as much water as the

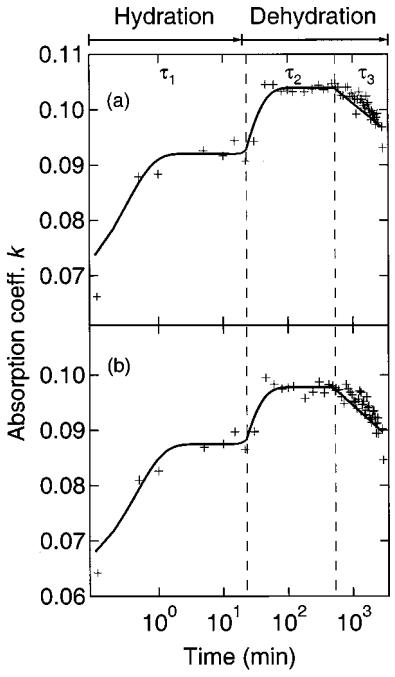

FIG. 5. Absorption coefficient k for a fingernail sample on a logarithmic time scale for two spectral regions, (a) 400–500 nm and (b) 500-600 nm. Three different time domains are discernible in both regions. The solid curves are exponential and linear fits, respectively. The sample was stored at room temperature for five weeks at 40% relative humidity.

sample used for the first hydration study, which was presented in Fig. 3. In the first part of the dehydration, the refractive index increases slowly compared to the decrease observed during hydration. This increase is even decelerated after some hours. When drying the sample for several days, the value of n reaches the starting level again. This dehydration behavior of the refractive index can be fitted with a double exponential function

$$n = C + D\exp\left(-\frac{t}{\tau_2}\right) + E\exp\left(-\frac{t}{\tau_3}\right). \tag{3}$$

The two time constants are $\tau_2 \approx 150$ min and $\tau_3 \approx 3200$ min in the wavelength range of 400–500 nm. Regarding just the first hour, the shape of the curve of n is similar to the ones presented in Fig. 3(b). Due to the high value of τ_2, the increase of n is invisible on the short time scale shown in Fig. 3(b). The same three time domains with the same critical time points are visible for k as well. The absorption coefficient shows an exponential increase while hydrating. The dehydration process must be separated into two steps. At the beginning, another exponential increase, instead of the expected decrease, appears. Hereafter, k decreases slowly in a linear manner.

In Fig. 6, we present a framework hypothesis that can account for the observed hydration dynamics. There are two states for water in bio-organic materials such as nails or stratum corneum, the topmost layer of skin: ''free'' and ''bound'' water (Ref. [15] denotes these states as ''low'' and ''high''

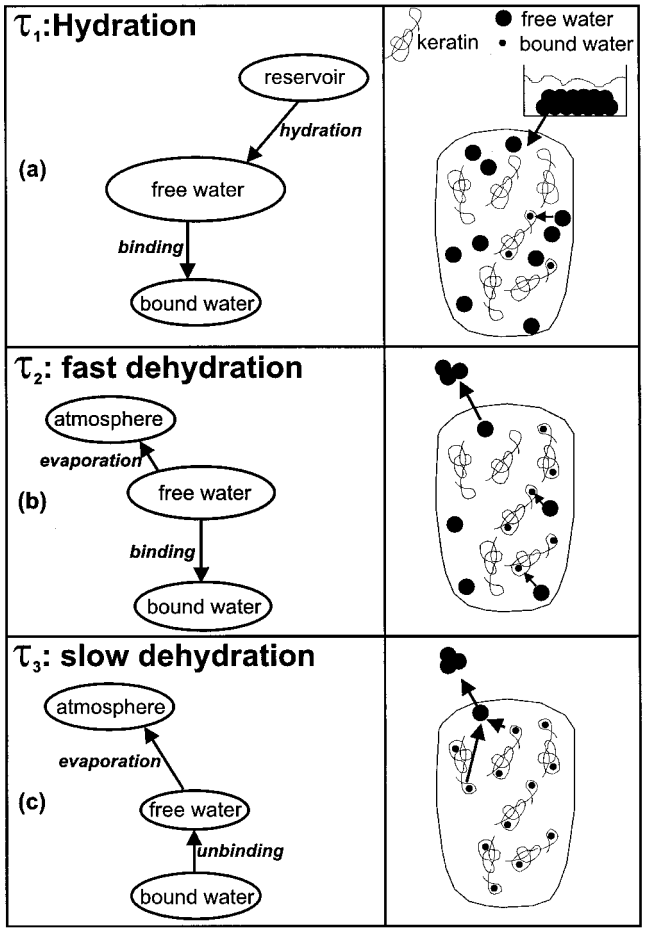

FIG. 6. A hypothesis for explaining the measured hydration dynamics in the human nail.

density water, Ref. [16] calls them ''free'' and ''structured'' water). The ''free'' water is only loosely bound into the nail structure, nearly like a mix of water and the other ingredients of the nail. ''Bound'' water is strongly interacting with the keratin matrix structure. The water molecules form crystal-like pentagonal structures around the proteins [16]. The ''bound'' water can influence the quartenary structure of the keratin or even the tertiary structure by shielding side chains of the amino acids. Apart from changing the conformation of the proteins, the ''bound'' water can also affect the structure of the keratin matrix, e.g., through forming hydrogen bonds. When a nail is hydrated as shown in Fig. 1, the incoming water is distributed into ''free'' and ''bound'' water [Fig. 6(a)]. After stopping hydration, the incorporation of ''bound'' water can continue, whereas the ''free'' water starts to evaporate into the air [Fig. 6(b)]. Once all ''free'' water has vanished into the air or into ''bound'' water, the latter starts to be released into ''free'' water that evaporates into the environment [Fig. 6(c)]. Within this framework, the refractive index is determined through the keratin-water mix, whereas the absorption coefficient, which is very low for water in the ultraviolet and visible spectral region [17], will be very sensitive to the above described conformational changes. We propose a simple numerical model of the dynamics of water

incorporation into the nail. The basic assumption is that water absorbed by the nail can be classified either as being ''free'' or ''bound.'' The water transport is assumed to go between the environment to the ''free'' state, and between the ''free'' and the ''bound'' state, but not directly between the ''bound'' state and the environment:

$$(H_2O)_{env} \rightleftharpoons (H_2O)_{free} \rightleftharpoons (H_2O)_{bound}. \tag{4}$$

The exchange of water between the three states is assumed to be driven by concentration differences described by rate equations,

$$\frac{dN_{free}}{dt} = \alpha_1(N_{env} - N_{free}) + \alpha_2(N_{bound} - N_{free}),$$

$$\frac{dN_{bound}}{dt} = \alpha_2(N_{free} - N_{bound}). \tag{5}$$

The constant α_1 is the exchange rate between the environment and the ''free'' state, α_2 describes the exchange between the ''free'' and the ''bound'' states. The parameters N_{env}, N_{free}, and N_{bound} are normalized measures of the water contents in the environment, ''free,'' and ''bound'' states, respectively. Unity represents full saturation of the respective water types. N_{env} was set to unity during hydration and zero during dehydration. It is reasonable to assume that the exchange rate of water between the nail and the environment is drastically different when the nail is immersed in liquid water and when the nail is surrounded by air. Therefore, the constant α_1 was allowed to be different during hydration and dehydration. To include the stability of the keratin-water complexes in the model, the constant α_2 was allowed to depend on the direction of the net flow of water between the ''bound'' and ''free'' states. The coupled Eqs. (5) were solved numerically with the initial condition $N_{free}(0) = N_{bound}(0) = 0$ to give the time dependence of the amounts of water in the two different states in the nail. The computed hydration dynamics is displayed in Fig. 7(a) for one selection of parameters, shown in Table I. The optical constants have been derived from $N_{free}(t)$ and $N_{bound}(t)$ assuming that the optical properties of the nail can be determined from its constituents using the effective medium approximation [6]. We use three constituents for our model, namely, (1) a basic host material describing the uninfluenced parts of the nail, (2) ''free'' water incorporated into the nail structure, and (3) ''bound'' water-keratin complexes. For a heterogeneous system of one host material and one embedded material, the complex refractive index $\tilde{n}_{eff}$ can be determined from Eq. [6]

$$\tilde{n}_{eff}^2 = \frac{(1+2q)\tilde{n}_h^2\tilde{n}_e^2 + 2(1-q)\tilde{n}_h^4}{(1-q)\tilde{n}_e^2 + (2+q)\tilde{n}_h^2}, \tag{6}$$

where $\tilde{n}_h$ and $\tilde{n}_e$ are the complex refractive indices of the host and embedded material, respectively, and q is the volume fraction of embedded material. In our case, we have three constituents of our effective medium, which was solved by invoking Eq. (6) recursively. First, an intermediate medium was constructed from constituent (2) with embeddings of (3) using $q = N_{bound}/(N_{free} + N_{bound})$. Second, this intermediate medium was used as an embedded material in the host material (1) with a volume fraction $q = (N_{free} + N_{bound})/(N_{free} + N_{bound} + 1)$.

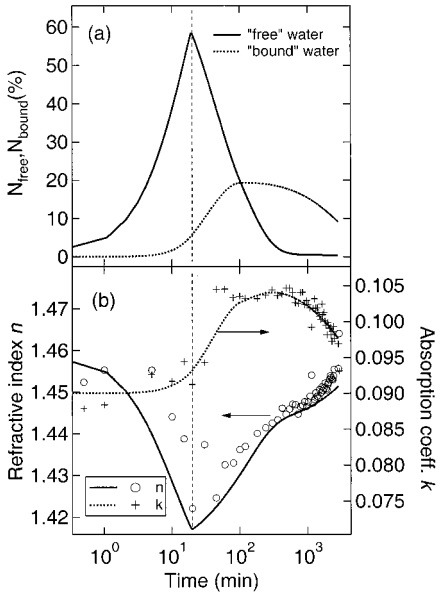

FIG. 7. (a) Calculated time dependence of the water concentrations in the ''free'' and ''bound'' states. (b) Corresponding optical constants and the experimental values from Figs. 4(a) and 5(a). The vertical dashed line marks the change from hydration to dehydration.

The time-dependent optical constants n and k as obtained from the model are depicted in Fig. 7(b). The measured refractive index n and absorption coefficient k are very well reproduced by the simple model. Especially the existence of two time domains during dehydration is clearly visible in the figure. The crossover at $t \approx 100$ min between these two domains occurs roughly when the net flow of water between

TABLE I. Input parameters used to produce the curves in Fig. 7 and Fig. 8.

Hydration dynamics parameter	Value (ellipsometric) (min^{-1})	Value (weighing) (min^{-1})
α_1 (hydration)	0.05	0.058
α_1 (dehydration)	0.009	0.023
α_2 (''free''→''bound'')	0.009	0.004
α_2 (''bound''→''free'')	0.0003	0.0003

Effective medium parameter	Value (ellipsometric)
n_{host}	1.46
k_{host}	0.09
n_{free}	1.36
k_{free}	0.09
n_{bound}	1.36
k_{bound}	0.18

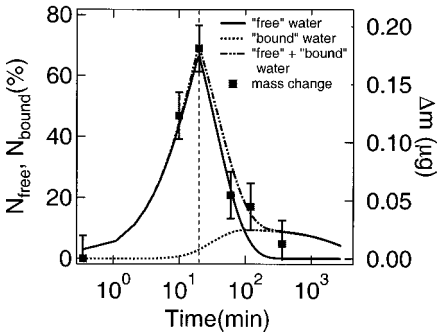

FIG. 8. Mass change in the probed sample volume during hydration and dehydration and calculated water concentrations. The vertical dashed line marks the change from hydration to dehydration.

''free'' and ''bound'' states is reversed, as can be seen by comparing Figs. 7(a) and 7(b).

The calculated optical parameters in Fig. 7(b) are not a result of a fitting procedure, rather they come from a specific choice of simulation parameters that can be found in Table I. It is fair to assume that the absorption coefficient of water is negligibly small. Since ''bound'' water is influencing the conformation of the protein, it is reasonable that the absorption coefficient of the nail is mainly governed by the amount of ''bound'' water, while the refractive index is affected by the presence of both types of water. The exchange of ''free'' water between the nail and the environment is much faster than the exchange of water between the ''free'' and ''bound'' states.

In addition one can confirm our model by measuring the change of the nail mass during hydration and dehydration. If one considers the effective sample volume of only 1.6×10^6 μm^3 in our ellipsometry measurements, one can estimate that the expected change of the nail mass is roughly 100 ng. Therefore, we collected three nail clippings from a different volunteer with an absolute mass of 62 mg and an estimated volume of 8.1×10^{10} μm^3. Assuming homogeneous physical properties, we derive the mass change in the probed sample volume as shown in Fig. 8. As one can see, the results of the weighing measurements can also be described with our model. During dehydration the shoulder especially can be well described by assuming a model with ''free'' and ''bound'' water. The parameters for this simulation can also be found in Table I.

Even though the agreement between the experimental data and the simulations is striking, one needs to consider that at present we have no means to determine the refractive index and the absorption coefficient of the constituents. The agreement between the simulated and measured optical constants provides evidence for the previously outlined hypothesis that the hydration dynamics of a fingernail is governed by the exchange of ''bound'' and ''free'' water, as well as the exchange of ''free'' water between the nail and the environment. In comparison with the model, we can identify the fast and slow dehydration processes as the release of ''free'' and ''bound'' water, respectively. In addition, we also derived the water profiles of ''free'' and ''bound'' water from the simulation as shown in Fig. 7(a). Additional weighing measurements showed similar features as can be seen by comparing Fig. 7(a) and Fig. 8.

IV. CONCLUSIONS

Ellipsometry has emerged as a very fruitful technique to study biological samples in a noninvasive way. The very low power density allows accurate measurements that hardly influence the sample. Spectra can be accumulated in short time intervals, so that one can resolve even relatively fast processes like the hydration of nails.

Apart from individual and biological variations, we are able to retrieve information about the optical parameters of human nails. The refractive index has typical values of 1.40 at a wavelength range of 400 to 600 nm. The absorption coefficient exhibits typical values of 0.06 and 0.10 at wavelengths of 700 and 450 nm, respectively.

We find that the optical constants of the nail change upon hydration and dehydration. This allows us to follow the water dynamics in real time. The hydration process is characterized by a time constant of about 4 min, while the dehydration process exhibits two distinct time domains with much longer time scales of 150 and 3200 min, respectively. Using the effective medium approximation, together with a numerical model that accounts for two types of water incorporation, we reproduce the time dependence of the complex refractive index during hydration and dehydration. From the simulation we derive the water profiles of ''free'' and ''bound'' water. The findings show that the hydration and dehydration properties of human fingernails can be fully described by the presence of two types of water.

ACKNOWLEDGMENTS

We thank U. Merkt, M.V. Klein, L. Börjesson, S. L. Cooper, J. Swenson, and M. Käll for many discussions. We acknowledge financial support for this work via BDF and DFG Ru773/2-1.

[1] R. R. Anderson and J.A. Parrish, J. Invest. Dermatol. **77**, 13 (1981).
[2] K. Hoffmann, K. Kaspar, P. Altmeyer, and T. Gambichler, Dermatology **201**, 307 (2000).
[3] T.L. Troy and S.N. Thennadil, J. Biomed. Opt. **6**, 167 (2001).
[4] V.V. Tuchin, S.R. Utz, and I.V. Yaroslavsky, Opt. Eng. **33**, 3178 (1994).
[5] S. Wessel, M. Gniadecka, G.B.E. Jemec, and H.C. Wulf, Biochim. Biophys. Acta **1433**, 210 (1999).
[6] R.M.A. Azzam and N.M. Bashara, *Ellipsometry and Polarized Light* (Elsevier, New York, 1999).
[7] W.L. Kerr, R.J. Baskin, and Y. Yeh, Eur. J. Physiol. **416**, 679 (1990).
[8] D.J. Brink and M.E. Lee, Appl. Opt. **37**, 4213 (1998).

[9] N. Shahidzadeh, D. Bonn, J. Meunier, and A. Mavon, Phys. Rev. E **64**, 021911 (2001).
[10] F.P. Bolin, L.E. Preuss, R.C. Taylor, and R.J. Ference, Appl. Opt. **28**, 2297 (1989).
[11] H. Lodish, D. Baltimore, A. Berk, S. L. Zipursky, P. Matsudaira, and J. Darnell, *Molekulare Zellbiologie* (Walter de Gruyter, Berlin, 1996).
[12] J.C. Garson, F. Baltenneck, F. Leroy, C. Riekel, and M. Muller, Cell. Mol. Biol. Lett. **6**, 1025 (2000).
[13] In order to use focusing optics one needs to integrate Eq. (1) over the angle of incidence spread determined by the effective *f* number of the focusing and collimation lens. However, performing measurements on calibrated Si samples with several numerical apertures, we confirmed that the impact of the lenses on n and k is less than 10^{-2}.
[14] D. De Berker, F. Wojnarowska, L. Sviland, G.E. Westgate, R.P. Dawber, and I.M. Leigh, Br. J. Dermatol. **142**, 89 (2000).
[15] P.M. Wiggins, Cell Biol. Int. **20**, 429 (1996).
[16] I.L. Cameron, K.M. Kanal, C.R. Keener, and G.D. Fullerton, Cell Biol. Int. **21**, 99 (1997).
[17] J.D. Jackson, *Classical Electrodynamics* (Wiley, New York, 1975), p. 291.